THE DYNAMIC ATMOSPHERIC AND AEOLIAN ENVIRONMENT OF JEZERO CRATER, MARS

C. E. Newman, *Aeolis Research, Chandler, AZ, USA (claire@aeolisresearch.com)*, **R. Hueso,** *UPV/EHU, Bilbao, Spain*, **M. T. Lemmon,** *SSI, College Station, TX, USA*, **A. Munguira,** *UPV/EHU, Bilbao, Spain*, **Á. Vicente-Retortillo,** *CAB, INTA, Madrid, Spain*, **V. Apestigue,** *INTA, Madrid, Spain*, **G. Martínez Martínez,** *LPI, Houston, TX, USA*, **D. Toledo Carrasco,** *INTA, Madrid, Spain*, **R. Sullivan,** *Cornell, Ithaca, NY,* USA, **K. Herkenhoff,** *USGS Astrogeology Science Center, Flagstaff, AZ, USA*, **M. de la Torre Juárez,** *JPL-Caltech, Pasadena, CA, USA*, **M. I. Richardson,** *Aeolis Research, Chandler, AZ, USA*, **A. Stott,** *ISAE-SUPAERO, Toulouse, France*, **N. Murdoch,** *ISAE-SUPAERO, Toulouse, France*, **A. Sanchez-Lavega,** *UPV/EHU, Bilbao, Spain*, **M. Wolff,** *SSI, College Station, TX, USA*, **I. Arruego Rodriguez,** *INTA, Madrid, Spain*, **E. Sebastián,** *CAB, INTA, Madrid, Spain*, **S. Navarro,** *CAB, INTA, Madrid, Spain*, **J. Gómez-Elvira,** *CAB-INTA, Madrid, Spain*, **L. Tamppari,** *JPL-Caltech, Pasadena, CA, USA*, **D. Viúdez-Moreiras,** *CAB, INTA, Madrid, Spain*, **J. Pla-Garcia,** *CAB, INTA, Madrid, Spain*; *SSI, Boulder, CO, USA*, **Mars 2020 Atmospheres Working Group**.

Introduction:

Aeolian processes are the main causes of change to the Martian surface and atmosphere in the modern era *(1,2)*. Large dust storms hugely alter atmospheric temperatures, densities, and circulation, presenting hazards to robotic and human missions, but atmospheric dust is present year-round, affecting visibility and solar power *(3,4)*. Yet, despite their importance to science and exploration, processes that move sand and raise dust have not been well quantified in situ, with missions lacking the necessary sensors and/or a sufficiently active aeolian environment *(5-12)*.

By contrast, the Perseverance rover carries the most sophisticated atmospheric and dust sensors yet flown to Mars. The Mars Environmental Dynamics Analyzer (MEDA; *13*) includes novel Radiation and Dust Sensors (RDS), which detect dust clouds and dust devils via changes to direct and scattered sunlight every second, simultaneous with MEDA measurements of p, T, wind and RH, and radiative fluxes from MEDA's Thermal InfraRed Sensor (TIRS). In combination, RDS and TIRS downward and upward SW radiation data provide albedo and albedo changes due to surface dust removal or deposition. These sensors allow MEDA to track the passage of dusty phenomena around / over the rover for a large fraction of each sol, and to relate it both to meteorological timeseries and surface changes. Perseverance also carries the first microphones to operate on Mars, providing data on turbulence, vortices, and wind activity *(14)*, and high-resolution cameras including the Navcams and Mastcam-Z, to image aeolian activity and features, such as dust devils and surface wind streaks *(15,16)*. Most crucially, Jezero crater contains many aeolian surface features, imaged both from orbit *(17,18)* and since landing, and dozens of examples of aeolian activity have been observed over the first 216 sols of the mission, covering early spring through early summer (L_s ~13-105°), as described below. The Mars 2020 mission is thus a perfect combination of instrumentation and environment for studying atmospheric and aeolian connections.

Results:

Wind patterns and aeolian surface features are controlled by regional and local slopes. In situ wind data confirm atmospheric model predictions *(19,20)* that Jezero crater wind directions are driven mainly by regional (Isidis basin) and local (crater rim) slope flows, resulting in a reversal of wind direction twice per sol. Daytime wind speeds vary hugely on sub-hourly timescales due to convective activity, but both hourly mean and maximum values are generally much stronger than those at night (Fig. 1A).

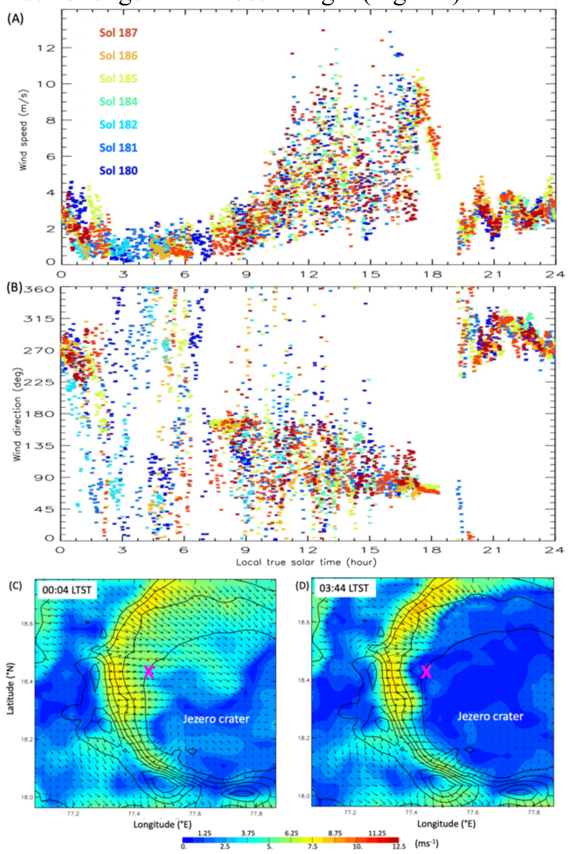

Fig. 1. Minute-average MEDA horizontal (A) wind speed and (B) direction at 1.45m at L_s~90°. (C,D) Modeled change in crater rim downslope flows from 00:04 to 03:44 LTST at L_s~90° using the MarsWRF mesoscale model.

Winds blow on average from the ESE from mid-morning through sunset (Fig. 1B), and are more southerly earlier and more easterly later in the day. The pattern of daytime winds is very similar to that predicted by both atmospheric models that resolve the crater slopes and those that do not (*19*). This suggests daytime winds are driven mainly by deep, strong, regional Isidis basin upslope flows, with limited impact of crater slopes during the daytime, when a thick planetary boundary layer (PBL) means flows are not confined close to the surface. However, closer inspection and comparison with modeling reveals a slight decrease in wind speed mid-afternoon, attributed to local crater slopes and associated flows.

Although wind stress (hence the ability to transport sand or raise dust, if available) increases with atmospheric density, which is greater at night, the dominance of daytime wind speeds over those at night translates to net sand transport towards 276° - i.e., from slightly south of east - over the first 216 sols of the mission. This sand transport direction is consistent with orbital observations of active sand transport from the ~ESE in and around Jezero crater *(17,18)* and with Perseverance observations of wind tails in Navcam and Mastcam-Z images (Fig. 2A,B).

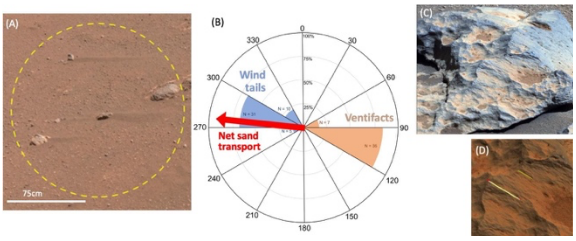

Fig. 2. (A) "Wind tails" (as seen in this Navcam image) indicate wind-driven sand transport directions. (B) Rose diagram showing orientations of wind tails (blue) and ventifacts (orange) seen along the rover traverse, plus net sand transport estimated from MEDA winds and densities over the first 216 sols (red arrow). (C) Ventifact seen by Mastcam-Z. (D) Example of azimuth measurements of flutes, used to infer the transport direction of abrading grains.

At night, winds since landing blow on average from the WNW, similar to the expected directions of nighttime downslope flows on both the Isidis and Jezero slopes. While Isidis slope flows are predicted to increase in strength until sunrise, however, the observed wind minimum around 03:00 LTST is only found in atmospheric models that resolve Jezero crater's rim (*19,20*). In such models (Fig. 1C,D) the rim blocks the regional downslope flows, which are relatively shallow due to a thin PBL at night, but develops its own strong downslope winds; these flows extend to the rover's current location earlier in the night but then intensify and concentrate on the rim after ~01:30, causing wind speeds to decrease at the rover's location, consistent with observations. As Perseverance drives to the crater rim, we expect nighttime wind speeds to increase greatly, which may result in dominant nighttime aeolian activity and net sand transport from the WNW.

Fluting in ventifacts observed by Perseverance along its traverse (Fig. 2C,D) already indicates dominant transport from the WNW (Fig. 2B), which is consistent with nighttime wind directions but inconsistent with wind stresses being larger during the daytime at all locations to date. This suggests the ventifacts formed during anomalous weather conditions (e.g. major dust storm) or a past climate epoch.

Rare 'gust lifting' events are linked to the passage of convection cells. In Perseverance's first 216 sols, Navcam took 30 time-lapse movies and 49 surveys (five image triplets taken all around the rover) designed to search for dust devils and dust lifting. Of these, three surveys show dust lifting by non-vortex wind gusts. Figs. 3 and 4 show data from the largest event, on sol 117. Based on the relationship of dust clouds to surface features (Fig. 3A), the first, north-centered triplet (Fig. 3B-D) shows dust being lifted over ~30s in a line ~N to S. Areas of active dust lifting cannot be clearly differentiated from those with dust blowing over them, but we estimate a lifting area of >4 km^2. The fifth image triplet (not shown), taken 5 mins later and centered just N of W, shows a dust cloud moving away over the delta to the NW of the rover, consistent with the observed wind direction and estimated delta height wind speed.

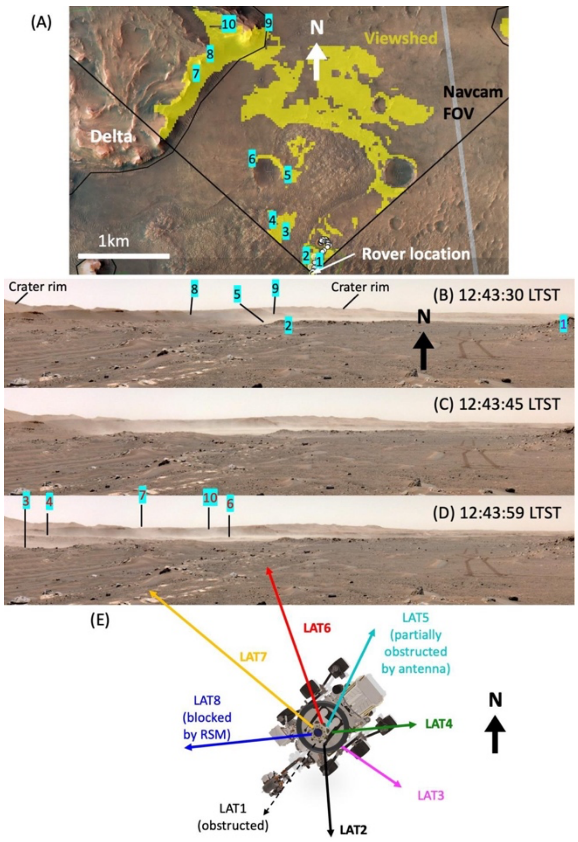

Fig. 3: (A) Surface features and viewshed. (B-D) The first, N-centered triplet of Navcam images (trimmed), 14s apart. (E) Azimuthal pointing of MEDA RDS sensors on sol 117.

Data from MEDA's RDS photodiodes (Fig. 4C) provide a more complete picture of this event. The vertical FOV of the lateral sensors is ~20-30° above the horizontal, with azimuthal pointing as in Fig. 3E, hence their signals can be interpreted as follows: Dust is raised and forms low dust clouds, producing the small lat6 and larger lat7 initial peaks; as lifting ceases, the dust is blown away at low altitudes to the WNW, moving sideways out of the lat6 FOV and below the lat7 FOV; as the cloud reaches the delta front, it rises and moves fully into the lat7 FOV, then moves below it again as it continues traveling away from the rover, producing the large, long, and smooth second lat7 peak. Other peaks are likely due to dust raised by a previous gust front passing the rover to the S/SW or diffuse dust activity to the E.

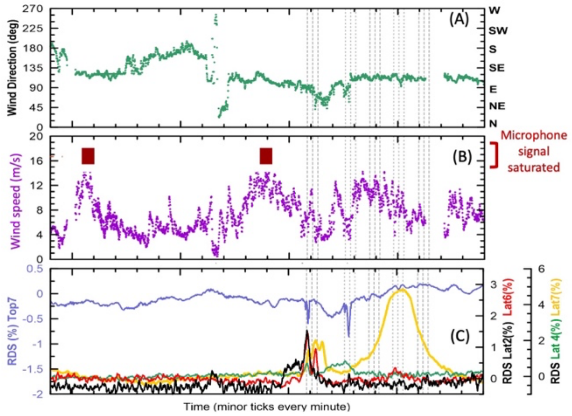

Fig. 4: MEDA (A) wind direction, (B) speed, and (C) RDS for 20 mins covering the sol 117 Navcam survey. Timing of the five image triplets is shown as vertical dotted lines.

All imaged gust lifting events to date occurred during the period of strong convective activity from ~10:30-16:00 LTST, which manifests as large temporal variability in wind speed (Fig. 1A; 4B), temperature, and other meteorological timeseries. On sol 117 this included a sequence of 24 SuperCam microphone recordings. The microphone signal is sensitive to the product of wind speed and its standard deviation (*21*) and two recordings made during the largest peaks in the MEDA wind data were strongly saturated (Fig. 4B), indicating particularly intense and variable winds. The timescale of the variations is consistent with the walls of convection cells passing overhead ~4-7 times per hour (periods of 8.6 to 15 minutes), advected by large-scale daytime upslope winds. Similar activity was reported for the InSight landing site *(22,23)*, but with fewer peaks per hour, and has long been predicted for Mars, both by analogy with Earth's deserts *(24)* and in Large Eddy Simulations (LES) *(25,26)*. These cells consist of strong, warm updrafts concentrated in narrow cell walls and weaker, cooler downdrafts in cell centers, with surface winds blowing toward the walls to conserve mass. As convection cells are advected over the region, the background and cellular near-surface winds have the same direction behind the leading cell wall and combine constructively to produce peak wind speeds there. This is also seen in the wind field of the MarsWRF mesoscale simulation (Fig. 5A). We thus suggest that gust lifting events are triggered by strong winds aligned in gust fronts behind the leading wall of strong convection cells, with these fronts (on average) perpendicular to the background wind direction. This is consistent with the pattern of dust lifting and transport seen on sol 117.

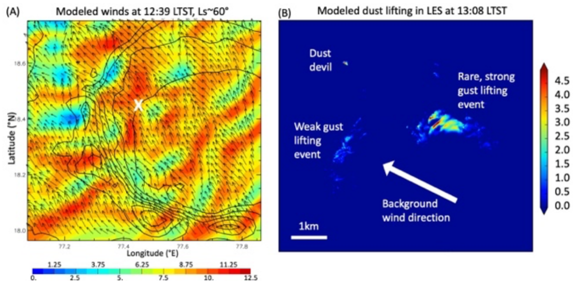

Fig. 5. (A) As in Fig. 1D but now showing daytime convection cells advected over Jezero at Ls~60°. (B) Snapshot of lifted dust flux in a MarsWRF LES of Jezero.

Output from the high-resolution MarsWRF LES is used to calculate dust lifting for a threshold wind stress of 0.008 Pa, and shows similar gust lifting events occurring along gust fronts (Fig. 5B). We speculate that a gust front responsible for the second large wind gust shown in Fig. 4B intensified shortly after it passed the rover, exceeding the threshold wind and producing the observed dust lifting. These results suggest 'gust lifting' in Jezero is produced by gust fronts with wind speeds exceeding a threshold that is some unknown amount greater than 15 ms^{-1}.

Daytime convective vortices and dust devils are common in Jezero crater. While dust lifting by wind gusts appears relatively rare, dust lifting by convective vortices is very common, with dust devils in 30% of movies and surveys designed to seek them (e.g. Fig. 6), and frequently in other images also.

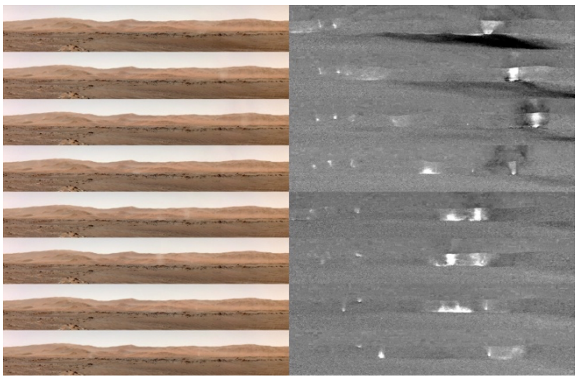
Fig. 6. (left) Frames every 28s from a Navcam dust devil movie at ~12:10 LTST on sol 148. (right) Difference between each image and the average, enhancing changes.

The signature of all passing convective vortices is highly distinctive in wind and pressure and often in temperature and longwave flux. Further, MEDA's RDS photodiodes allow us to identify those vortices with significant dust content. See the abstract of Hueso et al. for more details. Correcting for gaps in coverage, results show on average >4 daytime vortex pressure drops of >0.5 Pa per sol, with a peak of

>1.15 vortices per hour from 12:00-13:00 LTST. Of these vortices, ~25% produced a decrease in RDS top7 signal of greater than 0.5%, indicating sufficient dust content to significantly block incoming sunlight. This is a lower bound on the percentage of dusty vortices, due to the sun-rover-vortex geometry. However, even 25% would make Jezero's vortices far dustier than those observed by other missions.

Dustier vortices typically have larger pressure drops and maximum wind speeds, which are expected to be correlated *(27)*. This is consistent with stronger tangential winds - perhaps combined with a pressure drop 'suction' effect - producing greater dust lifting. Exceptions may have passed on the side of the rover opposite the sun and thus only appear to be less dusty. However, we find little correlation between the approximate vortex diameter and the pressure drop or dust content of the vortex.

Applying the same technique to InSight data, we find the peak number of vortex pressure drops >0.5 Pa from Ls~13-105° is nearly 2 per hour. However, if we correct for InSight daytime winds being ~twice as fast as in Jezero (hence vortices are blown past ~twice as fast), we find nearly as many vortices are *produced* at InSight as in Jezero. We also find a similar distribution of vortex diameters and intensities. Peak pressure drops >8Pa were found during the equivalent seasonal period at InSight *(28)*, compared to a peak of ~6.5Pa in Jezero, while peak vortex-associated wind speeds up to 31ms^{-1} were found at InSight *(12)*, similar to the 32ms^{-1} in Jezero. At both sites, these were inferred to cause surface changes seen in imaging, such as motion of surface grains and appearance of nearby dust devil tracks at InSight *(11,12)*, or the appearance of surface grains on the rover deck and motion of surface drill tailings at Perseverance. Yet puzzlingly, InSight never imaged a single dust devil, in stark contrast to Perseverance.

Local dust lifting was detected (via RDS/TIRS albedo changes) four times in association with vortex passage, providing direct data on threshold conditions needed to raise dust. We find no local dust lifting by vortices for tangential wind speeds < 15 ms^{-1} or central pressure drops < 2.6 Pa. This minimum wind speed for dust lifting is comparable to that measured regularly in association with passing convection cells, yet such speeds alone have not been observed to raise dust locally, suggesting the vortical nature of the encounter may be important. See the abstract of Vicente-Retortillo et al. for more details.

Discussion:

Dust devils and wind gusts could contribute equally to background dust lifting. An outstanding question for Mars is what maintains the background dust haze: dust devils or lifting by non-vortical wind stress. We find that >30% of dust devil surveys / movies clearly contain dust devils, while gust lifting events were found in <4% of surveys / movies. However, the huge sol 117 gust lifting event may have raised dust over >4 km^2. By contrast, we estimate the largest dust devil imaged would have swept out an area 1/10th as large. While the other two gust lifting events were far smaller, and larger dust devils were inferred from MEDA data, it is feasible that dust lifted by gust fronts might have equaled that lifted by vortices over this period, unless events such as that on sol 117 are very rare. More data are needed to assess this and to look for seasonal variations.

Significance for understanding threshold conditions for dust lifting. A related question is what threshold conditions must be exceeded for sand motion or dust lifting to occur. We find local dust lifting by vortices occurs only for winds > ~15 ms^{-1}, which was also the minimum reported by *(12)* at which surface darkening (inferred as dust lifting by a passing vortex) was observed at InSight. However, winds of 15 ms^{-1} have been observed at some point by most surface missions to carry wind sensors *(11,12,29-31)* but have not been observed to raise dust outside of vortex encounters, or to move sand. While Perseverance measured wind speeds of 15ms^{-1} shortly before imaging huge gust lifting activity, no dust was raised locally. Combined with a lack of similar events either imaged or detected by MEDA RDS in most periods with similarly strong wind speeds, we assume that the gust front strengthened after passing over the rover, hence the winds associated with dust lifting are unknown. Thus a notional 15 ms^{-1} threshold appears limited to dust lifting by a vortex, which may involve additional (e.g. pressure drop) effects.

Why is Jezero crater so active compared to most other landing sites? The ability of gust fronts associated with convection cells to - albeit rarely - raise large amounts of dust differs from observations at all prior landing sites. Further, the fraction of vortices that are dusty is far higher than at all previous sites for which this fraction was known. The contrast with InSight is particularly striking, as it has equivalent size, number, and intensity of vortices to Jezero, but has yet to definitively detect any dust devils. Identifying the cause of this difference, such as surface properties affecting dust lifting, will have major implications for understanding dust lifting across Mars.

References: [1] Diniega et al. *Geomorph.* (2021). [2] Szwast et al. *JGR* (2006). [3] Viúdez-Moreiras et al. *JGR* (2019). [4] Kahre et al. *Atmos. & Climate of Mars* (2017). [5] Baker et al. *GRL* (2018). [6] Sullivan et al. *JGR* (2008). [7] Moore et al. *USGS Prof. Paper 1389* (1987). [8] Greeley et al. *JGR* (2010). [9] Kahanpää et al. *JGR* (2016). [10] Viúdez-Moreiras et al. *Icarus* (2019). [11] Charalambous et al. *JGR* (2021). [12] Baker et al. *JGR* (2020). [13] Rodriguez-Manfredi et al. *SSR* (2021). [14] Chide et al. *Icarus* (2021). [15] Maki et al. *SSR* (2020). [16] Bell et al. *SSR* (2021). [17] Chojnacki et al. *JGR* (2018). [18] Day & Dorn *GRL* (2019). [19] Newman et al. *SSR* (2021). [20] Pla-García et al. *SSR* (2020). [21] Morgan & Raspet *JASA* (1992). [22] Spiga et al. *JGR* (2021). [23] Lorenz et al. *Icarus* (2021). [24] Spiga *GIMDS* (2012). [25] Richardson et al. *JGR* (2007). [26] Michaels & Rafkin *QJRMS* (2004). [27] Renno et al. *JAS* (1998). [28] Lorenz et al. *Icarus* (2021). [29] Martínez et al. *SSR* (2017). [30] Bridges et al. *JGR* (2017). [31] Viúdez-Moreiras et al. *Icarus* (2019).